Titanium-Rich Mineral Phases and the Nucleation of Bainite

J.M. GREGG and H.K.D.H. BHADESHIA

Experiments have been conducted to study the nucleation of bainite at interfaces between ceramic compounds of Ti and low-alloy steel. To facilitate this, chemically pure compounds of Ti were pressure-bonded to steel samples. The resulting composite samples were then heat-treated to induce transformation and, hence, to compare transformation behavior in the vicinity of the ceramic/steel interface to that within the bulk of the steel. It is found that a variety of Ti oxides are effective in stimulating the nucleation of bainite, whereas TiN is not. The results are interpreted in terms of the crystal structure and chemistry of the Ti compounds.

I. INTRODUCTION

HIGHLY organized microstructures can often be found in steels. Ferrite can, for example, grow in the form of packets containing parallel plates, which are in the same crystallographic orientation.[1] Cleavage cracks, or deformation processes, can therefore extend across the packets, the effects of the individual plates being minimal as far as mechanical properties are concerned.

Some of the most exciting recent developments in wrought and welded steel technology have involved acicular ferrite.[2] Far from being organized, this microstructure is better described as chaotic. The plates of acicular ferrite nucleate heterogeneously on inclusions and radiate in many different directions from these "point" nucleation sites.[3,4] Propagating cleavage cracks are therefore frequently deflected as they cross an acicular ferrite microstructure. This, obviously, is beneficial to mechanical properties.

Bainite and acicular ferrite are essentially identical in transformation mechanism,[5-8] the difference in morphology arising because the former nucleates at austenite grain surfaces (and hence tends to grow in organized packets), whereas the latter grows in many directions from inclusions. The inclusions are, therefore, the key to the break up of packets.

A large number of experiments[9-16] indicate that inclusions rich in Ti are most effective in acicular ferrite production. A number of different mechanisms have been proposed. It is rare, however, that the specific Ti compound responsible for the observed effects is identified. This is because many of the compounds have similar crystal structures and lattice parameters; when microanalysis is used, elements such as C, N, and O are either undetectable or cannot be estimated with sufficient accuracy to determine the stoichiometric ratio with respect to Ti. In reality, the nonmetallic inclusions tend to consist of many crystalline and amorphous phases[4,11,13-15,17-21] so that it becomes difficult to identify the particular component responsible for nucleation of acicular ferrite.

These difficulties prompted Strangwood and

Bhadeshia[7] to conduct controlled experiments in which pure ceramic phases were pressure-bonded to steel in order to create interfaces that could be studied with confidence. Effective ceramics should cause enhanced transformation in the vicinity of the interface when compared with the reaction within the bulk of the steel. Because of the lack of adequate equipment, high-hardenability steels were used so that only allotriomorphic ferrite formation could be examined. Here, we report new experiments using a low-alloy steel to study specifically the role of Ti compounds in stimulating bainite (and hence acicular ferrite).

II. EXPERIMENTAL METHOD

The composition of the low-alloy steel used is shown in Table I. Unless otherwise stated, Alloy 1 was used. Its relatively high Si content suppresses the formation of carbides, which might themselves cause heterogeneous nucleation. The Mn and C concentrations give sufficiently high hardenability to allow bainite to form without interference from higher temperature reactions such as the allotriomorphic ferrite transformation. The alloys were received in the form of $\sim$10-mm-diameter rods. These were reduced by machining down to 8-mm-diameter rods. The bainite start temperature (B_S) of the alloy was estimated using a method described elsewhere.[22] A more accurate value was obtained by isothermal transformation experiments at temperatures close to the calculated start temperature, after austenitization at 1200 °C for 10 minutes. All heat treatments were performed using a *Thermecmaster* thermomechanical simulator. The equipment is computer controlled, with computer data collection. The sample is heated by a radio frequency (RF) coil, in an environmental chamber. Standard thermal and mechanical treatment involves spot welding a Pt-Rh thermocouple to the steel specimen and placing it between the two ram heads within the specimen chamber. The ram heads are then lowered so that the specimen is held in position, surrounded by the RF induction heating coil. The chamber is then evacuated to a pressure of $\sim$2 $\times$ 10^{-2} Pa before commencement of the computer-controlled thermal and mechanical treatment. Microstructural observations showed that bainite was produced during transformation at temperatures up to $\sim$540 °C, with Widmanstätten ferrite occurring at higher temperatures. The B_S temperature was therefore identified experimentally to be close to

J.M. GREGG, Postgraduate Research Student, and H.K.D.H. BHADESHIA, Reader in Physical Metallurgy, are with the Department of Materials Science and Metallurgy, University of Cambridge, Cambridge CB2 3QZ, United Kingdom.

Table I. Chemical Composition of the Steels Used

Alloy	C (Wt Pct)	Si (Wt Pct)	Mn (Wt Pct)	Mo (Wt Pct)	Al (Wt Pct)	O (ppm)	N (ppm)
Alloy 1	0.204	1.95	1.54	0	0.01	8	7
Alloy 2	0.30	0.15	<0.02	4.20	0	—	—

~540 °C, which compares with the calculated value of ~560 °C.[22]

High-purity powders of TiN, TiO, Ti_2O_3, and TiO_2 were obtained from various chemical synthesis companies. The Ti compound was placed between two 6-mm lengths of the steel rod, as shown in Figure 1. In some of the early experiments, the center of the lower cylinder was drilled out to a depth of 2 mm to accommodate the mineral powder. In later experiments, this was deemed unnecessary, as it involved extra machining and produced a less intimate steel-mineral interface. Using the Thermecmaster, the steel-mineral assembly was heated to 1200 °C for 10 minutes, during which a compressive load of 400 N (~8 MPa) was applied. This was found to be sufficient to cause the mineral and steel to bond. After the 10 minutes at high temperature, the load was removed and the specimen was gas-quenched (using either He or N) at ~40 °C s^{-1} to 510 °C s^{-1} (i.e., below B_S). It was held for 25 seconds at this temperature before further gas quenching to room temperature.

The bonded specimens were then sectioned in a plane normal to that of the ceramic/steel interface using a Struers Accutom-2 precision high-speed saw. They were hot-mounted in conductive BAKELITE,* and prepared for metallography by grinding using SiC paper and polished using 6-μm diamond paste, before etching in 2 pct Nital. It was found that on some occasions, a part of the oxide that was originally bonded to the steel was removed during metallographic preparation. This is not a serious problem because most of the observations were on the steel, and in any case, many regions could be found where the oxide remained connected to the steel. Scanning electron microscopy (SEM) and microanalysis were carried out using CAMSCAN S2 and S4; the latter is equipped with an energy dispersive X-ray (EDX) analysis unit. Transmission electron microscopy (TEM) was conducted on a PHILIPS** 400T (with EDX), 400ST,

*BAKELITE is a trademark of Union Carbide Corporation, Danbury, CT.
**PHILIPS is a trademark of Philips Electronic Instruments Corp., Mahwah, NJ.

and JEOL 2000FX (with thin-windowed EDX).

III. RESULTS AND DISCUSSION

Each of the various combinations of ceramic and steel were found to be quite different in their response to heat treatment and are discussed separately.

A. Titanium Dioxide: TiO₂

Figure 2 reveals that the steel near the TiO_2 layer shows a lot more bainite than the bulk of the steel away
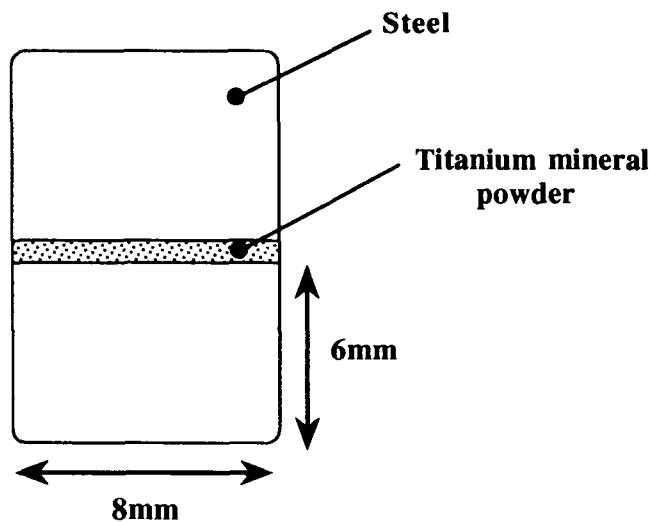

Fig. 1 — Schematic diagram of the steel-mineral arrangement.
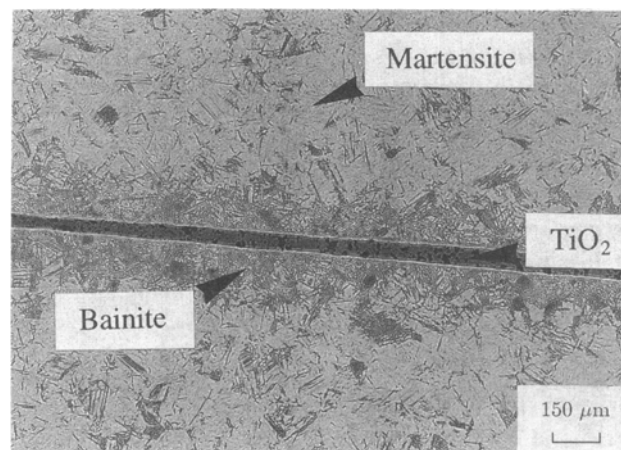

Fig. 2 — Optical photomicrograph of the TiO_2-steel interface region. There is clearly more bainite present adjacent to the mineral than elsewhere in the steel.

from the ceramic/steel interface. It would therefore appear to be very potent in nucleating bainite. Closer examination showed that the bainite does not emanate directly from the TiO_2-steel interface. The presence of TiO_2 causes the production of a zone of allotriomorphic ferrite ~15 to 20-μm thick (Figure 3), which contains amorphous spherical particles (Figures 4 and 5). These were found, using microanalysis, to consist almost entirely of Si and O. A typical EDX trace of these particles taken on TEM is shown in Figure 6. Such spherical particles are probably amorphous silica.

It is clear that O has diffused over a distance of some 20 μm from the TiO_2 into the steel. Similar effects were
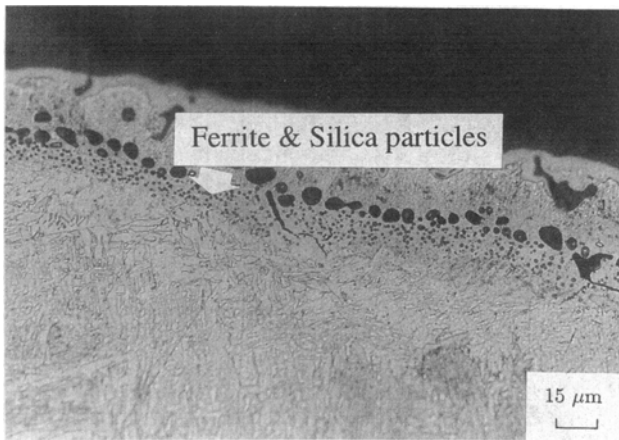
Fig. 3—Optical photomicrograph of the ferrite and SiO$_x$ particles produced adjacent to the TiO$_2$.
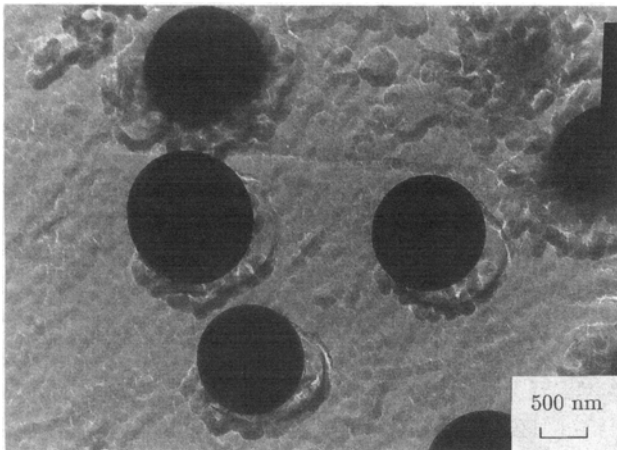

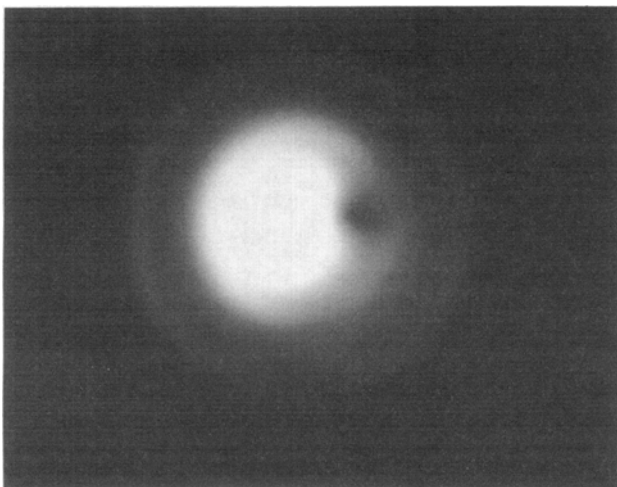Fig. 4—TEM photomicrograph of typical silica particles.

Fig. 5—Diffraction produced from a silica particle illustrating its amorphous nature.

not found at the surfaces of the steel that were not in contact with the ceramic, confirming that the observed phenomenon is induced by the ceramic (Figure 7).

In order to show that it is the property of TiO$_2$ to cause oxidation, which in turn induced the ferrite, silica, and bainite production, another O-producing mineral was tested in the bonding experiments—KNO$_3$ (a mineral that decomposes to give O at 400 °C).[23,24] The decomposition of KNO$_3$ produced bainite nucleation, as shown in Figure 8. The particle layer observable in the figure is composed predominantly of silica particles—the high Si content of these particles was observed using SEM EDX (Figure 9). These particles are contained within a ferrite layer (Figure 10). Thus, the decomposition of KNO$_3$, and consequential exposure of the steel to O, produced the same salient "reaction zone" features displayed at the TiO$_2$-Alloy 1 interface.
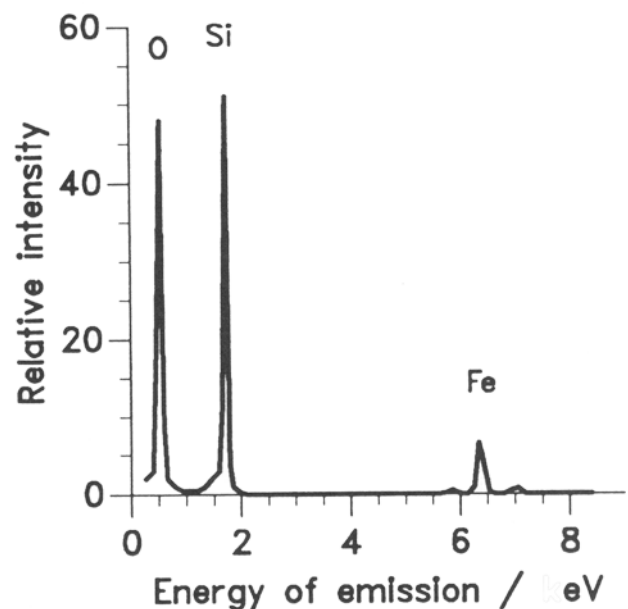

Fig. 6—TEM EDX trace (using thin-windowed detector) of the particles present in the ferrite layer produced adjacent to the TiO$_2$.
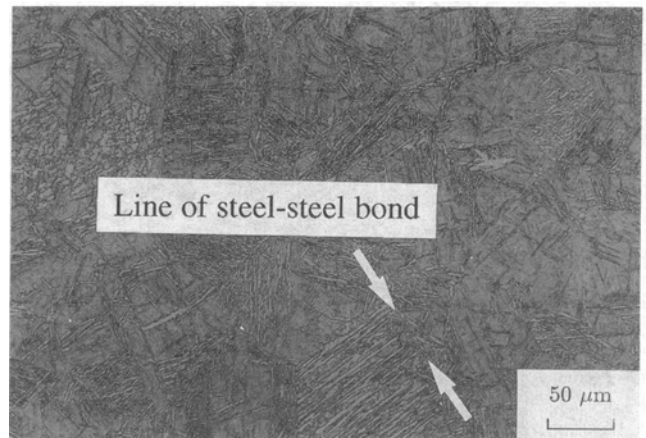

Fig. 7—Optical photomicrograph of a steel-steel interface produced by pressure bonding. As can be seen, no reaction zone is produced.
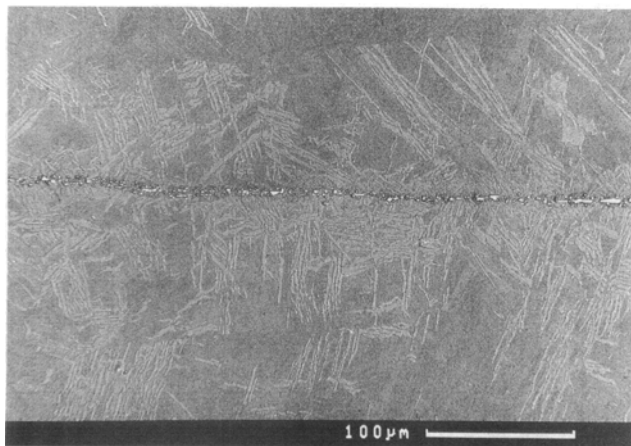
Fig. 8—SEM photomicrograph of the KNO_3-Alloy 1 interface showing the bainite produced local to the KNO_3. The observable particles are predominantly silica.
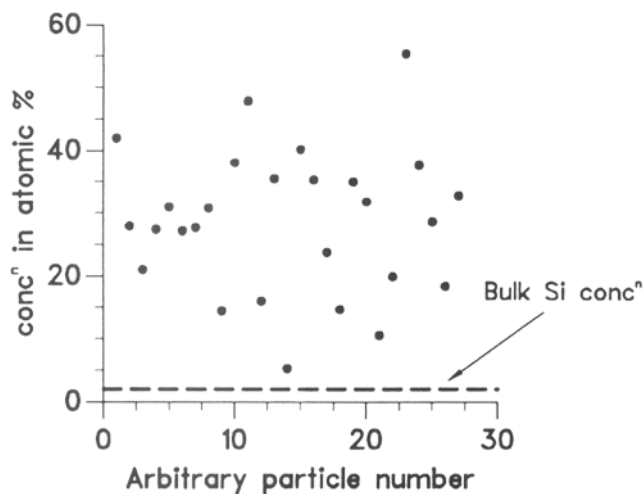

Fig. 9—SEM EDX results taken from particles in the KNO_3-steel specimen. As can be seen, they are highly enriched in Si.
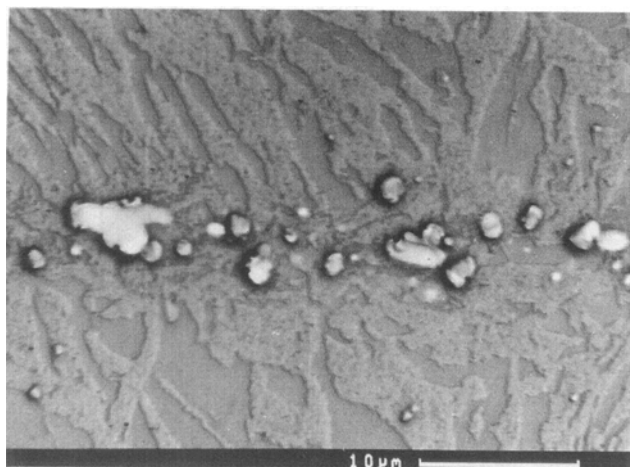

Fig. 10—SEM photomicrograph illustrating the ferrite layer that surrounds the Si-rich particles produced by the KNO_3.

Furthermore, exposure of the steel to water vapor at 1200 °C also caused a reaction zone adjacent to the free surface (Figure 11). It seems, therefore, that it is the ability of TiO_2 to cause oxidation of the local steel Alloy 1, which is responsible for the nucleation observed.

Line profiles of substitutional element concentrations were taken perpendicular to the TiO_2-steel interface in order to investigate any effects the O may have on steel hardenability. A typical observed profile can be seen in Figure 12. There is an apparent depletion of Mn and Si in the reaction zone adjacent to the TiO_2. The depletion of Si seems likely to be caused by the formation of the silica particles within this reaction zone. The depletion of Mn is likely to be caused by its expulsion from the growing allotriomorphic ferrite. For this to be so, a peak
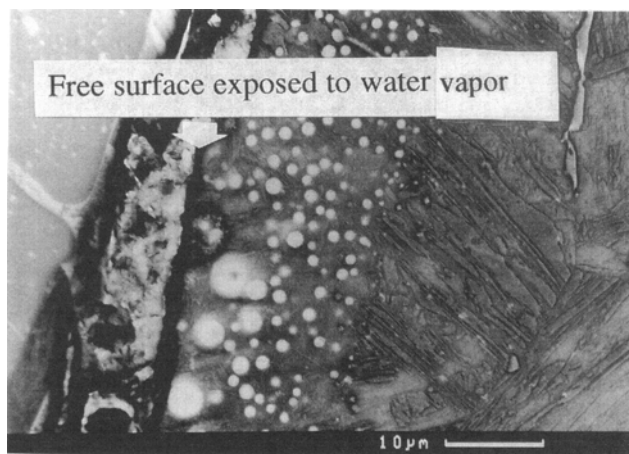

Fig. 11—SEM photomicrograph showing the reaction zone produced in steel adjacent to a surface that has been exposed to water vapor at 1200 °C.
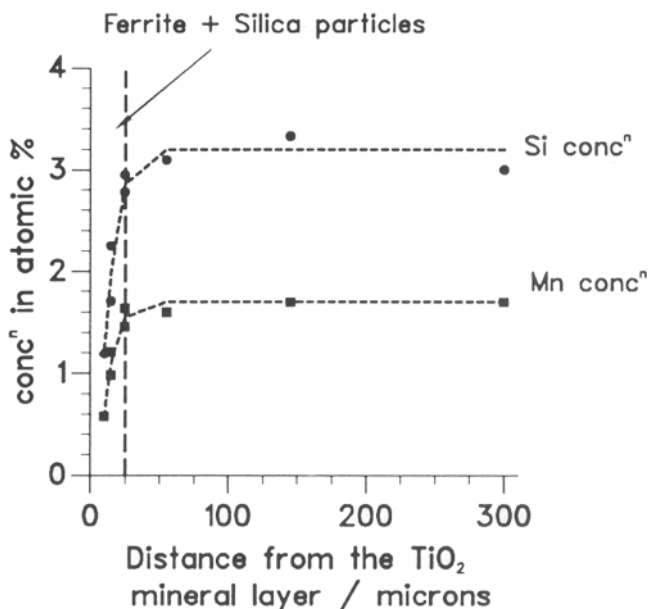

Fig. 12—SEM EDX line profile showing the variation in substitutional element concentrations with distance from the TiO_2 layer for Alloy 1.

in the Mn concentration beyond the ferrite/bainite interface would be expected. This cannot be observed. However, it should be noted that the SEM EDX system samples an area ~5 μm in diameter so that a peak in Mn will not be observable if situated close to a trough, since the peak and trough will be sampled, for the most part, simultaneously. It is suspected that the lack of observation of such a Mn peak is due to the poor resolution of the SEM EDX system. Apart from this substitutional depletion within the reaction zone, the O presence seems to have had no other effect.

Although the Si and Mn depletion may be explained by the formation of the ferrite and silica layer, it may be that the O presence affected the substitutional elements in the austenite prior to the formation of the ferrite. In order to investigate this possibility, TiO_2 was bonded to Alloy 1 at 1200 °C for 10 minutes, as before, and then water-quenched to room temperature. It was hoped that such rapid quenching would prevent the formation of any ferrite, so allowing observation of the effects on substitutional element concentrations produced due to the O penetration alone. As shown in Figure 13, the formation of a reaction zone was not totally suppressed, even at the cooling rates produced by water quenching (~400 °C/s).

The extent of growth of the reaction zone was, however, reduced to a mere 3 to 4 μm. Figure 14 shows that the Mn and Si were unaffected outside of the thin reaction zone, proving that the changes in concentration are caused by the formation of ferrite and silica, rather than by something that happens in the austenitic condition during heat treatment at 1200 °C. The O that penetrates the steel during the 1200 °C treatment precipitates silica, and it is speculated that it removes carbon from the austenite near the ceramic. This induces ferrite formation that rejects Mn as it grows.

To further validate this hypothesis and demonstrate that the formation of silica is not necessary for the production of bainite, a further experiment was conducted using a low-Si steel (Alloy 2, Table I).

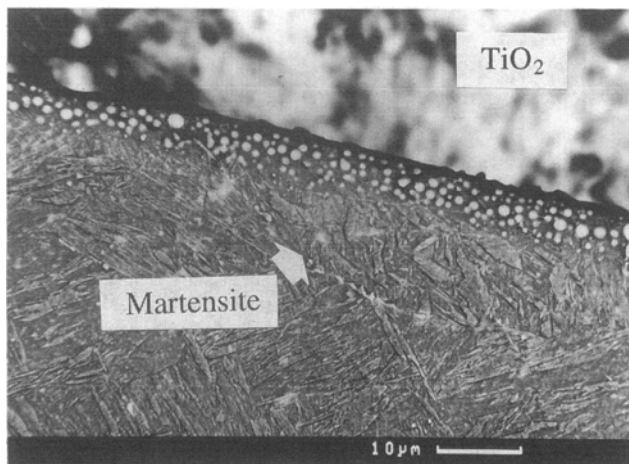The B_S of Alloy 2 was estimated in the same way as for the previous alloy, using the computer software followed by a series of isothermal transformations. For this alloy, the true Mo concentration was too high for the range of the computer program, and therefore, an estimated B_S was calculated on the basis of 1.5 wt pct Mo. This gave a B_S of ~570 °C. Experimentally, it was found to be ~510 °C in the 4.2 wt pct Mo alloy. Partial transformation of the bonded TiO_2-Alloy 2 specimens was performed at 480 °C for 55 seconds. This time, no reaction zone was found, nor was any layer of the allotriomorphic ferrite at the ceramic/steel interface. The oxide nevertheless stimulated for the formation of bainite (Figure 15).

A line profile of the concentrations of Si and Mo produced adjacent to the TiO_2 layer in Alloy 2 is shown in Figure 16. Because of the lack of any reaction zone in this alloy, the effects produced by oxidation alone may
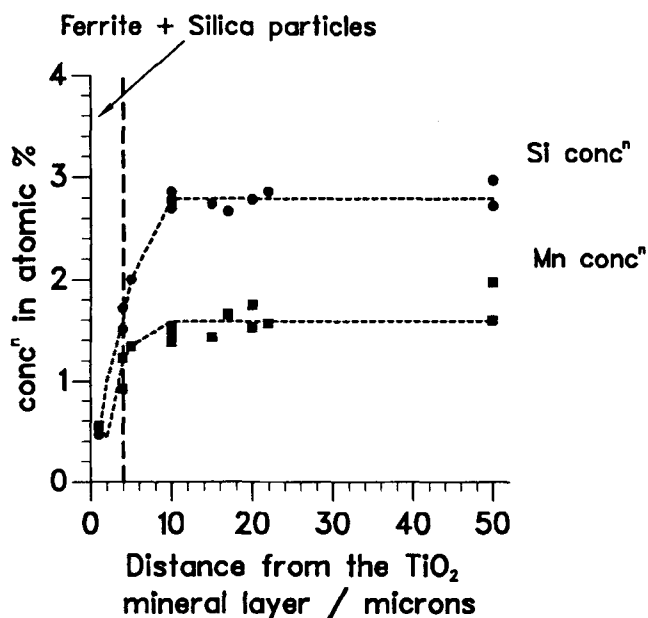

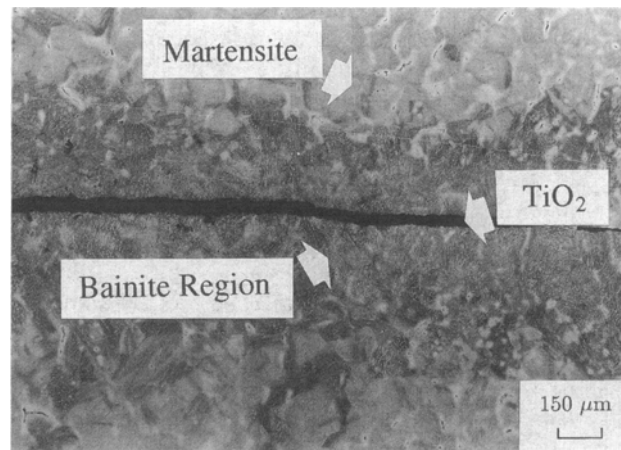Fig. 14—EDX profile showing the Mn and Si concentrations away from the TiO_2 layer in the water-quench experiment.

Fig. 13—SEM photomicrograph of the reaction zone produced adjacent to TiO_2 when water-quenched from 1200 °C. The ferrite and silica layer is still present, but its growth has been reduced to ~3 to 4 μm.

Fig. 15—Optical photomicrograph of the TiO_2-Alloy 2 interface region. Bainite is produced without the production of a ferrite and silica layer.
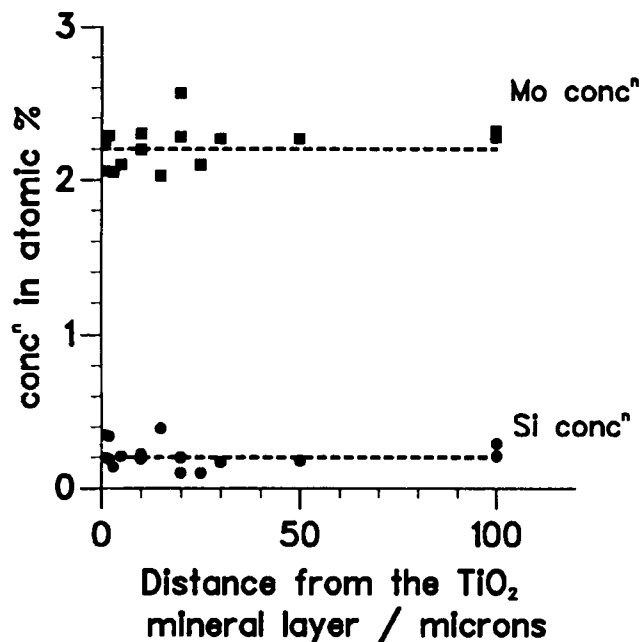
Fig. 16—EDX line profile of the Mo and Si concentrations away from TiO_2 in Alloy 2.

Fig. 17—SEM photomicrograph of the interface region between Ti_2O_3 and the steel. Bainite production is enhanced by the interface but without the production of a ferrite and particle layer.

be observed. Clearly, there is very little, if any, effect on the substitutional elements due to the presence of O.

So, it seems that TiO_2 induces nucleation of ferrite and bainite in the region of the steel adjacent to it by causing the diffusion of O into the steel. Such O presence seems to have little direct effect on the substitutional element concentrations within the steel; although, in Alloy 1, it did cause the formation of silica particles. However, as shown in Alloy 2, the presence of such silica particles is not necessary for the production of bainite. It is suggested that the O presence within the steel may induce decarburization, making the austenite more amenable to ferrite formation. The details of this hypothesis remain to be proven.

B. Titanium Sesquioxide: Ti_2O_3

The characteristics of the Ti_2O_3 as a stimulant for bainite nucleation were found to be similar to those of TiO_2 (Figure 17). However, the presence of Ti_2O_3 did not produce the layer of allotriomorphic ferrite nor any silica particles. Furthermore, SEM microanalysis revealed that the presence of Ti_2O_3 caused the long-range depletion of Mn in the steel local to the mineral layer. Figure 18 illustrates a typical concentration profile, which was verified on four separate occasions. Note that no Si depletion was observed, consistent with the absence of any silica particles.

Figure 19 shows that the oxide, in fact, is a sink for Mn; the associated depletion of Mn in the adjacent steel must then cause the enhanced formation of bainite.

Note that the scale of the Mn-depleted zone depends very much on the quantity of oxide available as a sink. Ti_2O_3 is often stated to be a good nucleant for acicular ferrite, but the particles involved are then rather small so that the scale of any depletion is expected to be much smaller by comparison.
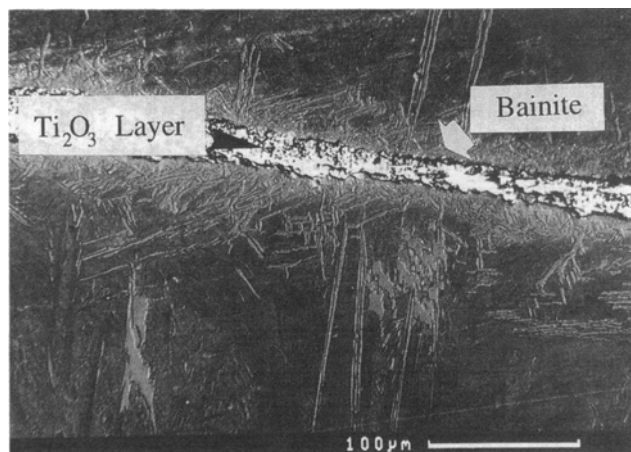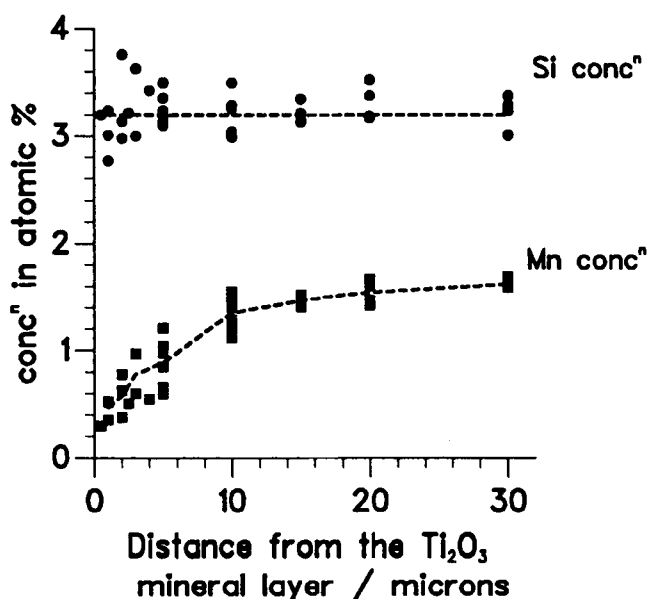

Fig. 18—SEM EDX concentration profile showing the relative depletion of Mn caused by the Ti_2O_3 mineral layer.

C. Titanium Nitride: TiN

The TiN-steel interface is shown in Figure 20. Under an optical microscope, it seems that this interface does not enhance the nucleation of bainite in the steel adjacent to it. The SEM examination confirms that little, if any, extra inducement for transformation occurs adjacent to TiN than elsewhere in the steel. Certainly, the level of bainite production caused by the TiN-steel interface is meager when compared with that caused by TiO_2 and Ti_2O_3-steel interfaces. It would, therefore, seem that TiN is not an active nucleant for the production of acicular ferrite in real steel systems. This is contrary to the suggestions of Barbaro et al.,[19] Watanabe and Kojima,[16] and Kluken and Grong.[21]

D. Titanium Monoxide: TiO

The TiO-steel combination is similar to the Ti_2O_3-steel interface, in that it induces the nucleation of bainite in
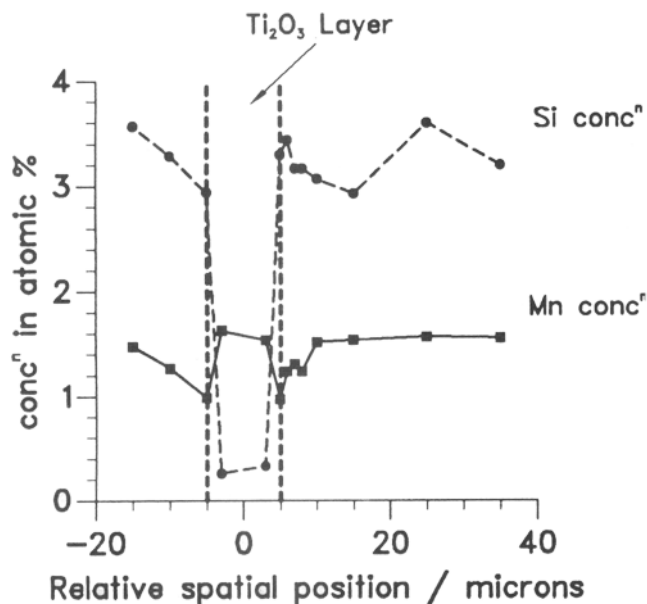
Fig. 19—SEM EDX concentration profile across the Ti_2O_3 layer showing the presence of Mn within this layer.
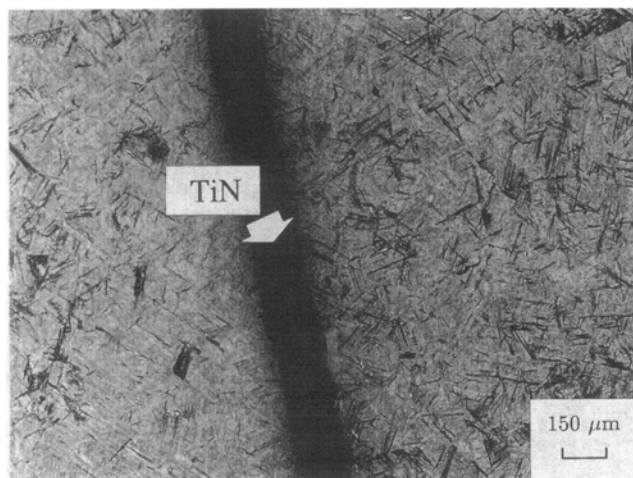

Fig. 20—Optical photomicrograph of the interface region between TiN and the steel. There is little, if any, extra inducement to form bainite adjacent to the TiN than elsewhere.
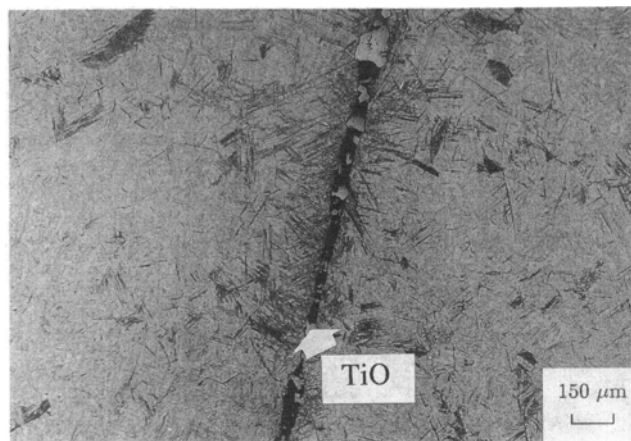

Fig. 21—Optical photomicrograph of the interface between TiO and the steel. Bainite nucleation adjacent to the mineral layer is evident, and no ferrite and particle layer has been produced.
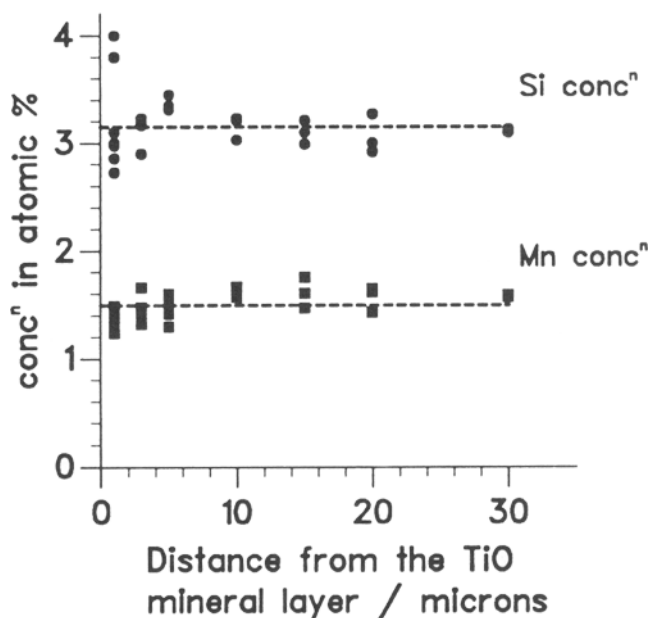

Fig. 22—SEM EDX concentration profile of substitutional elements in the steel with respect to the distance from the TiO layer.

the adjacent steel (Figure 21). There is also an absence of the layer of allotriomorphic ferrite and SiO_x particles that occurred with the TiO_2. However, unlike the Ti_2O_3, SEM EDX indicates that the presence of TiO does not significantly affect the substitutional solute concentration in the adjacent steel (Figure 22).

The observation that TiO does cause bainite nucleation from its surface is in agreement with earlier work[10,17] where it is argued that TiO is effective as a nucleant because it has a good lattice match with ferrite. In the present context, TiN also offers a good lattice match for ferrite and yet does not appear to enhance bainite nucleation.

The true mechanism by which TiO causes the nucleation of bainite when pressure-bonded to steel is, therefore, still under consideration and obviously requires

further investigation with a much wider range of minerals. Nevertheless, the bonding experiments have clearly shown that TiO may cause the nucleation of bainite from its surface. Table II summarizes some of the features of the Ti minerals tested in the bonding experiments. There are several points to note.

(1) Note the similarity in structure and lattice parameters between TiO and TiN. TiO does cause bainite nucleation in the context of these experiments, whereas TiN does not. If lattice matching between TiO and the ferrite structure causes it to nucleate bainite, then TiN should also be able to cause nucleation.

(2) The heat of formation of TiO_2 is less than that of Ti_2O_3. Thus, the production of O vacancy defects in TiO_2, the loss of O, and the eventual formation of Ti_2O_3 may be rationalized.

Table II. Summary of Some of the Properties of the Ti Minerals Tested in the Bonding Experiments[25–28]

Mineral	$-\Delta H_f^o$/kJ mol^{-1}	Melting Point (°C)	Boiling Point (°C)	Lattice Type	Lattice Parameters (Å)
TiO	518.7	1750	3000	cubic F	$a = 4.18$
Ti$_2$O$_3$	1520	decom. 2130	—	hex. P	$a = 5.15$, $c = 13.64$
TiO$_2$	941.0	1830 to 1850	2500 to 3000	tetr. P	$a = 4.59$, $c = 2.96$
TiN	305.4	2930	—	cubic F	$a = 4.24$

(3) TiO has a lower heat of formation than either TiO$_2$ or Ti$_2$O$_3$ and would therefore seem more likely to "react" with Alloy 1 than either of the other two oxides. This is contrary to our observations and indicates that the ability of the ceramic to react with steel requires more detailed analysis.

IV. SUMMARY AND CONCLUSIONS

A technique has been established that allows the systematic study of the ability of oxides and other compounds to stimulate the nucleation of bainite. Using this, it was demonstrated that TiO$_2$, Ti$_2$O$_3$, and TiO are all effective in enhancing the formation of bainite in the adjacent steel. The mechanism by which each compound stimulates ferrite nucleation is found to be different in detail.

1. TiO$_2$ appears to induce transformation by oxidizing the steel at elevated temperatures. Exactly how the oxidation process causes nucleation is not clear, but it may involve a decarburization of the steel.

2. Ti$_2$O$_3$ appears to act as a sink for Mn and, hence, causes a reduction of Mn levels in the steel that surrounds it. Manganese is known to retard the transformation of steel to ferrite, and so any depletion in the steel has the opposite effect.

3. TiO is found not to be reactive in the sense discussed in 2, nor does it act as a sink for elements such as Mn. It nevertheless enhances the nucleation of bainite, although the mechanism by which this happens is not clear since its lattice match with ferrite is similar to that of TiN, which does not stimulate bainite formation.

In contrast to these Ti oxides, TiN appears to show little efficacy in inducing bainite transformation in adjacent steel.

On the basis of these results, it would seem that it is Ti oxides and not nitrides that are important in causing the formation of acicular ferrite in welded and wrought steels. The mechanisms by which such oxides cause nucleation seem to be dependent on their stoichiometry.

ACKNOWLEDGMENTS

REFERENCES

1. H.K.D.H. Bhadeshia: in *Future Developments of Metals and Ceramics*, J.A. Charles, G.W. Greenwood, and G.S. Smith, eds., Institute of Materials, London, 1992, pp. 61-63.
2. H.K.D.H. Bhadeshia: *Bainite in Steels*, Institute of Materials, London, 1992.
3. D.J. Abson, R.E. Dolby, and P. Hart: *Weld. Inst. Res. Rep.*, 1978, vol. 67, 1978, p. M.
4. G.S. Barrite, R.A. Ricks, and P.R. Howell: *Quantitative Microanalysis with High Spatial Resolution*, The Metals Society, London, 1981, pp. 112-18.
5. A.A.B. Sugden and H.K.D.H. Bhadeshia: *Metall. Trans. A*, 1989, vol. 20A, pp. 1811-18.
6. J.R. Yang and H.K.D.H. Bhadeshia: in *Advances in Welding Technology and Science*, S.A. David, ed., ASM INTERNATIONAL, Metals Park, OH, 1987, pp. 187-191.
7. M. Strangwood and H.K.D.H. Bhadeshia: *Advances in Welding Technology and Science*, S.A. David, ed., ASM INTERNATIONAL, Metals Park, OH, 1987, pp. 209-13.
8. A.O. Kluken, Ø. Grong, and J. Hjelen: *Metall. Trans. A*, 1991, vol. 22, pp. 657-63.
9. H. Terashima and P.H.M. Hart: *Int. Conf. on the Effects of Residual Impurity and6Microalloying Elements on Weldability and Weld Properties*, The Welding Institute, London, 1983, Paper 27.
10. N. Bailey: *Weld. Inst. Res. Rep.*, 1983, vol. 221/1983.
11. J.M. Dowling, J.M. Corbett, and H.W. Kerr: *Metall. Trans. A*, 1986, vol. 17A, pp. 1611-23.
12. H. Homma, S. Ohkita, S. Matsuda, and K. Yamamoto: *Internal Report, Nippon Steel Corporation*, Chiba, Japan, 1986.
13. M. Es-Souni and P.A. Beaven: *Surf. Interface Anal.*, 1990, vol. 16, pp. 504-09.
14. M. Es-Souni, P.A. Beaven, and G.M. Evans: International Institute of Welding Document, No. 6, II-A-847-91, International Institute of Welding, Paris, France, 1991.
15. G. Thewlis: *International Institute of Welding Document*, No. IXJ 165 90, 1990, International Institute of Welding, Paris, France, pp. 1-11.
16. I. Watanabe and T. Kojima: *J. Jpn. Weld. Soc.*, 1980, vol. 49 (11), 772-80 and vol. 50 (7), pp. 702-09.
17. N. Mori, H. Homma, S. Okita, and M. Wakabayashi: International Institute of Welding Document, No.6IIW Doc IX 1196 81, International Institute of welding, Paris, France, 1981.
18. G.S. Barrite and D.V. Edmonds: *Advances in the Physical Metallurgy and Application of Steels*, The Metals Society, London, 1981, pp. 126-34.
19. F.J. Barbaro, R.H. Edwards, and K.E. Easterling: *7th Natl. Conf.*, Australian X-ray Analysis Association, University of Western Australia, Perth, Australia, 1988, vol. AXAA-88.
20. G. Thewlis: *Joining Mater.*, 1989, vol. 1, pp. 25-31 and vol. 2, pp. 125-29.
21. A.O. Kluken and Ø. Grong: *Metall. Trans. A*, 1989, vol. 20A, pp. 1335-49.
22. H.K.D.H. Bhadeshia: *Met. Sci.*, 1982, vol. 16, pp. 159-65.
23. N.V. Sidgwick: *Chemical Elements and Their Compounds*, Oxford University Press, London, 1950, vol. 1, p. 700.
24. N. Irving Sax: *Dangerous Properties of Industrial Materials*, Van Nostrand Reinhold Company, New York, NY, 1968, p. 1047.

25. *Handbook of Physics and Chemistry*, 57th ed., R.C. Weast, ed., CRC Press, Cleveland, OH, 61976.
26. *The Oxide Handbook*, G.V. Samsonov, ed., IFI/Plenum Data Corporation, New York, NY, 1973.
27. *Powder Diffraction Files*, Joint Committee for Powder Diffraction Studies, ed., International Center for Diffraction Data, Swarthmore, PA.
28. W.A. Deer, R.A. Howie, and J. Zussman: *An Introduction to the Rock Forming Minerals*, Longman Scientific and Technical, Essex, 1966.